

## INVESTIGATION OF LOW COST SMAs UNDER ELEVATED TEMPERATURES

**Sofia Piliafa<sup>1\*</sup>, Lazaros Melidis<sup>1</sup>, Lambros Kotoulas<sup>1</sup>, Nikolaos Makris<sup>1</sup> and Konstantinos Katakalo<sup>1</sup>**

<sup>1</sup> Aristotle University of Thessaloniki  
Laboratory of Experimental Strength of Materials and Structures, Thessaloniki, 54124  
e-mail: {spiliafa,kkatakalo}@civil.auth.gr, {lpkotoulas,nsvmakris}@gmail.com  
<https://strength.civil.auth.gr>

---

### Abstract

*Nowadays much emphasis has been placed on studying smart materials because of their ability to change their particular properties in a controlled manner by external stimuli. Shape memory alloys belong to the wider category of intelligent materials and exhibit two unique characteristic behaviors, superelasticity and shape memory effect, making them differ from conventional materials. These effects are due to diffusionless transformations between austenitic and martensitic phases. The SME occurs because a temperature-induced phase transformation reverses deformation and the pseudoelasticity achieves large, recoverable strains with little to no permanent deformation, as well, but it relies on more complex mechanisms. Innovative, low cost iron-based shape memory alloys (Fe-Mn-Si SMAs) with good workability, machinability, and weldability have been drawing much attention during the last two decades regarding to their potential application in engineering such as prestressing of concrete or coupling devices. In the present work we carried out experiments on monotonic mechanical loading, low-cycle fatigue and thermal loading in the laboratory of Experimental Strength of Materials and Structures of Aristotle University of Thessaloniki, so as to investigate in practice their behavior and all their special characteristics that already exist in the current literature.*

**Keywords:** low cost iron-based shape memory alloys, thermomechanical characterization, civil engineering applications.

---

## 1 INTRODUCTION

Shape memory alloys (SMAs) are metallic materials which belong to the wider category of smart materials. The last decades they have attracted the interest regarding to their potential application in engineering, due to their good mechanical properties including fatigue behavior, corrosion resistance and their ability to damp and absorb energy. [1-3] Shape memory alloys display two distinct crystal structures or phases (austenitic and martensitic phase), which depend on temperature and internal stress. Martensite exists at lower temperatures while austenite exists at higher temperatures. When an SMA is in martensite form at lower temperatures, the metal can easily be deformed into any shape. When the alloy is heated, it goes through transformation from martensite to austenite. In the austenite phase, the memory metal «remembers» its initial shape, before deformation [4]. Because of that, shape memory alloys exhibit two unique characteristic behaviors, superelasticity and shape memory effect. The loading–unloading cycle typically shows a pronounced hysteresis loop. In the shape memory effect, a large residual strain remains after unloading, which can be recovered by heating [5]. The two most prevalent shape-memory alloys are copper-aluminium-nickel and nickel-titanium (NiTi) which are preferable for most applications due to their stability and practicability [6]. However, low-cost, iron-based Shape Memory Alloys (Fe-Mn-Si SMAs) have been drawing much attention during the last three decades[7,8]. Fe-Mn-Si SMAs can be passive or active components in civil structures to reduce damage caused by environmental impacts or earthquakes [3]. Other possible applications of SMAs in civil engineering are passive vibration damping and energy dissipation, active vibration control, actuator applications, and the utilization of the SME (Shape memory effect) for prestressing or tensioning. Among those possible applications, the pre-stressing of structures using fixed shape memory alloys has attracted a considerable attention [8]. In contrast to conventional prestressing, neither anchoring systems nor hydraulic devices are necessary for applying the prestressing force, since prestressing is achieved by the shape memory effect produced by heating. This heating can be implemented by electrical resistance heating (Joule heating). However, to be suitable for prestressing, an SMA needs to have certain properties, such as a large and stable recovery stress [10,11]. The aim of this work is to broaden the knowledge of iron-based Shape memory alloys' mechanical behavior, which is now limited, through laboratory tests. The experimental work presented in this paper focuses on characterizing the thermo-mechanical response of the Fe-SMA through experiments on monotonic mechanical loading, low-cycle fatigue and thermal loading, carried out in the laboratory of Experimental Strength of Materials and Structures of Aristotle University of Thessaloniki. Stress and temperature were the investigation parameters.

## 2 MATERIALS AND METHODS

To characterize the thermo-mechanical response, four dog-bone shaped tensile specimens with a gauge length of 60 mm and cross-section of 1.5 x 9 mm<sup>2</sup> were prepared from the original (Fe-SMA) plate. (see table 1) Then, unidirectional mechanical tests were performed using the Instron tensile testing machine equipped with a climate chamber which can be operated in a temperature range between 20°C (RT-Room Temperature) and 250°C. Instron machine contains also an integrated static load cell of 50 kN capacity and the Bluehill software which gives us the results of an experiment in a diagram form of load – strain. (see figure 1) During the tests, the strain evolution was measured with a clip-on extensometer. The stress–strain behavior of the alloy was characterized by applying tensile mechanical loading and unloading, in the two first specimens, under displacement-controlled conditions with a loading rate of 1 mm/min. The

recovery stresses as a function of the temperature were also measured in strain-controlled tests in the two other specimens. Firstly, the samples were subjected to 4 and 1% tensile strain and then heated to 160 and 250°C, respectively, and subsequently cooled down to RT, keeping the gauge length constant during the whole experiment. In Table 1 we depict all details of the experimental sequence. The heating rate was set to 6°C/min. As far as cooling is concerned it was held in a physical way, so the coolest temperature reached was approximately 20°C and the cooling rate was slow. (see figure 2)

Table 1: Detailed information of experiments

Name	Dimensions (mm)		Loading	T (°C)	Target strain	Comments
	t	b				
<b>Specimen 1</b>	1.50	9.15	MUT* <sup>1</sup>	RT(=23)	Up to failure	
<b>Specimen 2</b>	1.56	9.68	LCF* <sup>2</sup>	RT	Strain 4‰	
	1.56	9.68	LCF	RT	Strain 9‰	
	1.56	9.68	LCF	RT	Strain 3.5%	
	1.56	9.68	LCF	RT	Strain 6.5%	
	1.56	9.68	MUT	RT	Up to failure	
<b>Specimen 3</b>	1.52	9.03	TL* <sup>3</sup>	160		Prestrain 4% & complete unloading
	1.52	9.03	MUT	RT	Up to failure	
<b>Specimen 4</b>	1.55	9.41	TL	250		Prestrain 1% & Complete unloading
	1.55	9.41	MUT	RT	Up to failure	

\*1Monotonic Uniaxial Tension, \*2Low Cycle Fatigue (n=3), \*3Thermal Loading (n=1)

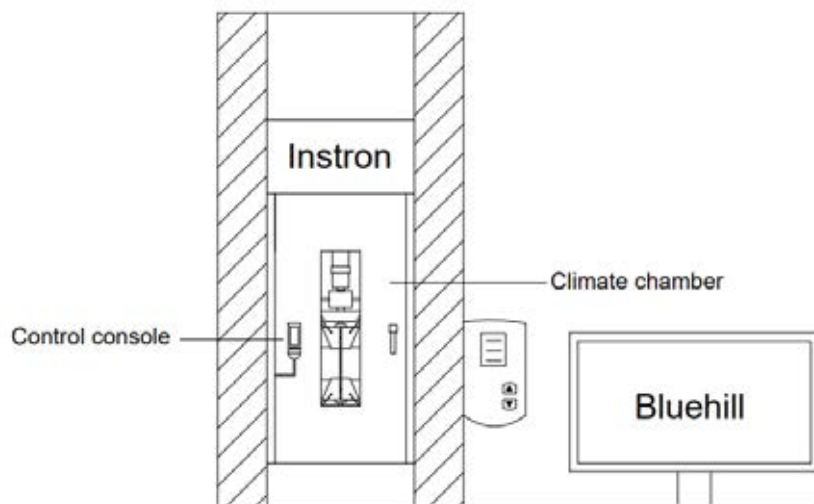


Figure1. Experimental setup with climate chamber

As mentioned before, the two first specimens (specimen 1 & 2) are tested under displacement-controlled conditions. Each one is placed carefully in suitable grips for its cross-

section, so as not to have slip losses and tension loads be applied right. Their dimensions are measured (1.5 x 9.15) mm and (1.56 x 9.68) mm, respectively, using a caliper. The first one is tested under monotonic, uniaxial tension loading up to failure. Specimen 2 is submitted to five low – cycle fatigue tests of three loading – unloading cycles with a different target strain each time. Target and residual strains of each cycle are given collectively in the table 2 below:

Table 2: Target and residual strains of each low-cycle fatigue test.

No of Cycle	Target strain	Residual strain
1st cycle	4‰	1.8‰
2nd cycle	9‰	5‰
3rd cycle	3.5%	2.8%
4th cycle	6.5%	5.8%

When four cycles are completed a gradual increase of loading is applied with the same rate of 1mm/min, as before.

Following the previous investigations, specimens 3 and 4 are tested in thermal loading. Each one is placed carefully in suitable grips for its cross-section, so as not to have slip losses and tension loads be applied right. Their dimensions are measured (1.52 x 9.03) mm and (1.55 x 9.41) mm, respectively, using a caliper. We have applied an initial pre-strain and total unloading to both specimens. When the protocol set is activated, the temperature starts increasing from 20°C (RT-Room Temperature) to the default values of 160 and 250°C with a rate of 6°C/min. When the heating is completed, the temperature is held for a few minutes, in order to achieve uniform temperature distribution in the specimen. When opening the climate chamber, cooling starts naturally and a Room Temperature of 20°C is reached. (details in table 3) After that, the extensometer is placed again, and monotonic uniaxial loading is forced to the specimen up to failure. Figure2 present the aforementioned thermal protocol.

Table 3: Required time for heating and cooling.

Target temp. (°C)		Heating time (min)	Constant time (min)	Cooling time (min)
Temp. (°C)	150	20	5	10
	260	60	5	40

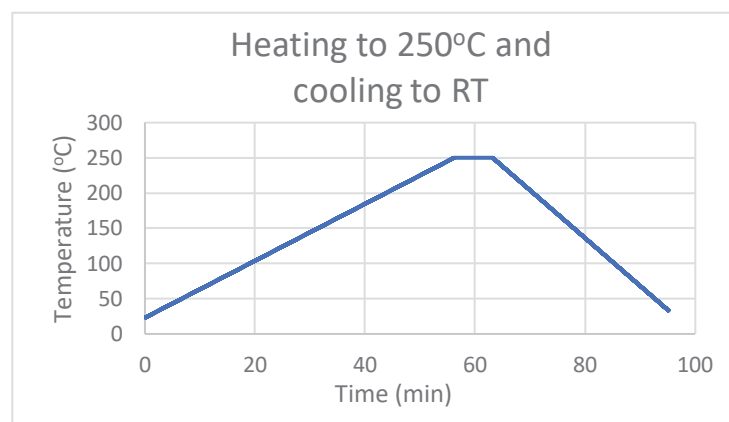


Figure 2: Time – Temperature diagram for heating to 250°C and cooling to RT

### 3 RESULTS

The following table 4 summarizes the results obtained from the experimental campaign occurred in the Laboratory for Strength of Materials and Structures.

Table 4. Summarized results

Name	Max. Load (kN)	Max. Stress (Mpa)	Max. Strain (%)	T (°C)	Residual strain (‰)
<b>Specimen 1</b>	13,734	1000	33	RT(=23)	Up to failure
<b>Specimen 2</b>	5,540	367	0,4	RT	1,8
	7,816	518	0,9	RT	5,0
	10,133	671	3,5	RT	29
	11,085	734	6,5	RT	58
	14,481	959	33	RT	Up to failure
<b>Specimen 3</b>	2,750	180	0,15	160	None
	9,230	672	35	RT	Up to failure
<b>Specimen 4</b>	3,870	250	0,19	250	None
	13,546	928	37	RT	Up to failure

Specimen 1 was monotonically loaded at room temperature up to failure. Figure 3 depicts the strain-strain graph of this coupon. An ultimate load of 13,734kN, which corresponds to 1000 MPa was recorded. The maximum measured strain was equal to 33%. It is obvious that at room temperature Fe-SMAs exhibit a high strength value together with high plasticity.

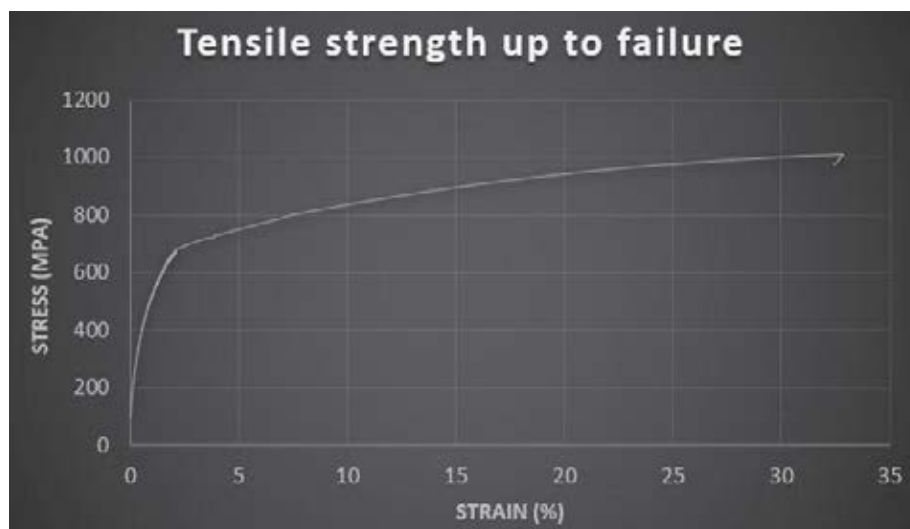
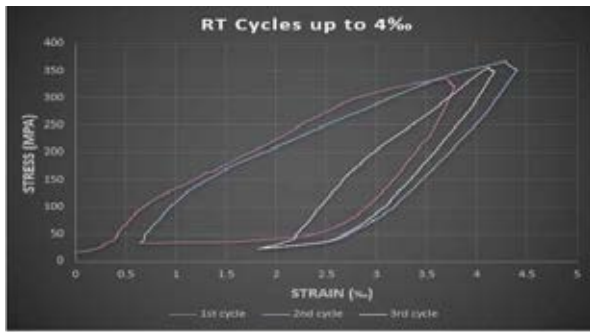
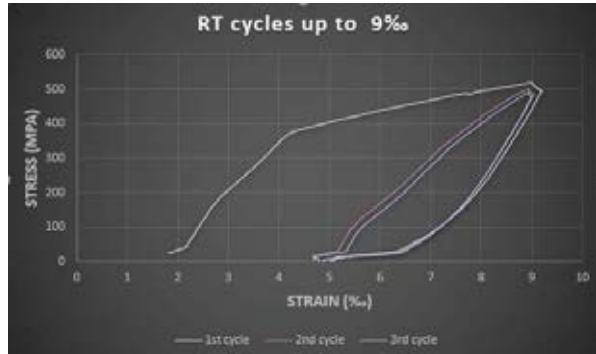
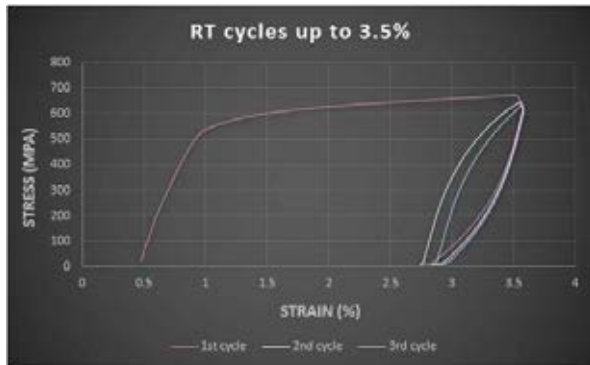
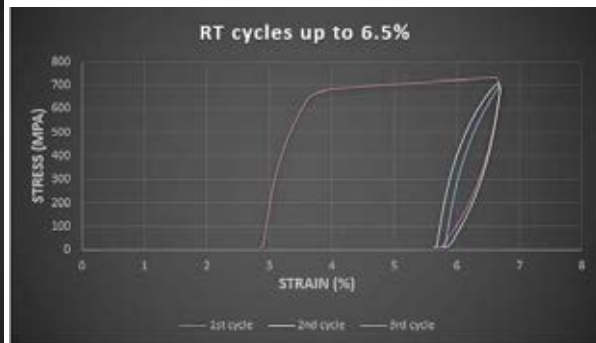


Figure 3.  $\sigma$ - $\epsilon$  graph for specimen 1

Specimen 2 was loaded for several cycles (see table 1), at room temperature but at different loading rates. The first 3 cycles were performed up to a strain limit of 4‰. The following at a strain limit of 9‰, value which was increased to 35‰ and 65‰. Finally, specimen 2 was loaded up to failure. Figures 4a to 4

Figure 4a.  $\sigma$ - $\epsilon$  graph for specimen 2 (4‰ target strain)Figure 4b.  $\sigma$ - $\epsilon$  graph for specimen 2 (9‰ target strain)Figure 4c.  $\sigma$ - $\epsilon$  graph for specimen 2 (35‰ target strain)Figure 4d.  $\sigma$ - $\epsilon$  graph for specimen 2 (65‰ target strain)

Concerning the pre-strain of 4‰ we noticed that the residual strain changed significantly when we slightly increased the target strain value, which means the investigated Fe-SMA is sensitive to the defined pre-strain value, leading to very different residual strains.

The further increase of the target strain from 4 to 9‰, leads to a gradient change of the  $\sigma$ - $\epsilon$  graphs' inclination (initial yield of the material), shortly after 4‰. The target strain remained stable to 9‰ at both three cycles, so loops follow a more regular behavior, having the same values of residual strains.

The following pre-strain levels are reaching 3.5% and 6.5% respectively. The mechanical behavior of alloy becomes clearly elastoplastic and the residual strains after unloading are becoming significant. (see figures 3c and 3d) Finally a loading-unloading sequence 12 cycles we applied monotonic uniaxial tension to the coupon specimen up to failure. When the sample reaches its fracture point stress of 959 MPa we measure an ultimate strain of 33%.

Comparing the overall behavior of specimen 1 and specimen 2 we could say that the loading-unloading of 12 cycles (low-cycle fatigue) did not affect the Fe-SMA's mechanical behavior.

Specimens 3 and 4 were used to investigate the thermomechanical behavior of the tested Fe-SMA's alloy. Specimen 3 was pre-strained to a level of 4% and was unloaded to RT conditions. A low stress of 25 MPa is kept constant to avoid grips' slip. Then the temperature was increased from RT to 160°C. When heating is activated a low increase of load is noticed which is soon decreased until we reached the target temperature of 160°C. From that temperature level until the cooling to room temperature (20°C) conditions, the load starts increasing. The increase of almost 180MPa depicts the prestress effect of the coupon. The aforementioned behavior is demonstrated in figure 5b. Similarly, specimen 4 was heated to 250°C and left to cool to RT. For the target temperature of 250°C we measured an imposed



stress equal to 250MPa. (see figure 6b). Finally, both specimens after the thermal loading-unloading were imposed to uniaxial tension up to failure. Figures 5a and 6a show the overall  $\sigma$ - $\epsilon$  behavior of the tested specimens 3 and 4.

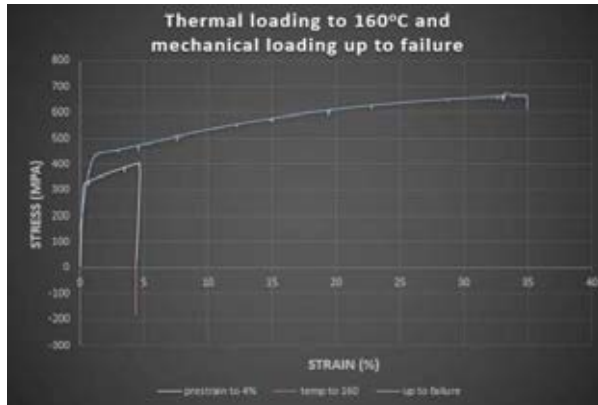


Figure 5a.  $\sigma$ - $\epsilon$  graph for specimen 3

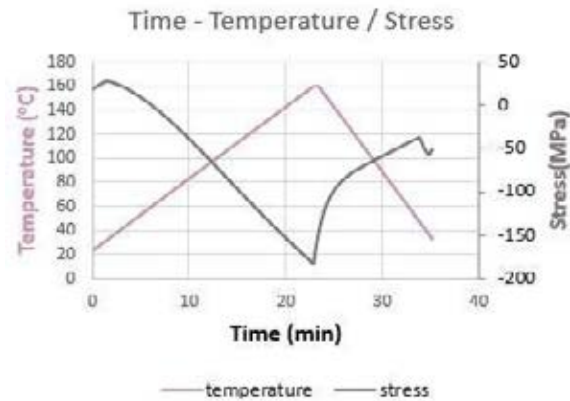


Figure 5b. Thermomechanical behavior of specimen 3

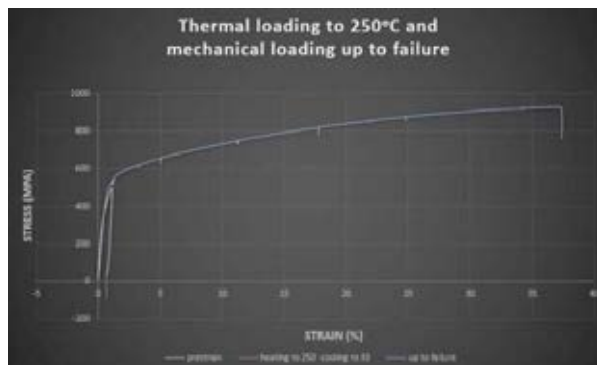


Figure 6a.  $\sigma$ - $\epsilon$  graph for specimen 4

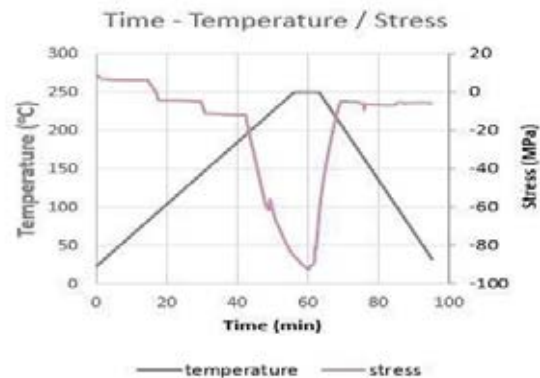


Figure 6b. Thermomechanical behavior of specimen 4

#### 4 CONCLUSION

- At room temperature Fe-SMAs exhibit a high strength value together with high plasticity.
- The investigated Fe-SMAs are sensitive to the imposed pre-strain value, leading to different residual strains
- The loading-unloading of 12 cycles (low-cycle fatigue) did not affect the Fe-SMA's mechanical behavior.
- Different levels of target temperature lead to different prestress levels

#### ACKNOWLEDGMENTS

Part of the aforementioned research “Investigation of the thermomechanical for smart materials to monotonic and low-cycle fatigue conditions” has been co-funded by Greece and

European Union through the Operational Program “EDBM-103: SUPPORT FOR RESEARCHERS EMPHASIZING YOUNG RESEARCHERS – 2<sup>nd</sup> CYCLE” (project code: 5047899) which are gratefully acknowledged.



## REFERENCES

- [1] L. Janke , C. Czaderski , M. Motavalli and J. Ruth ,Applications of shape memory alloys in civil engineering structures - Overview, limits and new ideas, Materials and Structures 2005
- [2] G. Songa, N. Maa, H.-N. Lib ,Applications of shape memory alloys in civil structures, Engineering Structures (2006)
- [3] A.R. Khaloo1 , P. Piran Aghl2 , I. Eshghi3, APPLICATION OF SMA IN CONCRETE STRUCTURES
- [4] [https://depts.washington.edu/matseed/mse\\_resources/Webpage/Memory%20metals/how\\_shape\\_memory\\_alloys\\_work.htm](https://depts.washington.edu/matseed/mse_resources/Webpage/Memory%20metals/how_shape_memory_alloys_work.htm)
- [5] W.J. Lee, B. Weber ↑ , C. Leinenbach, Recovery stress formation in a restrained Fe–Mn–Si-based shape memory alloy used for prestressing or mechanical joining, Construction and Building Materials (2015)
- [7] A. Arabi-Hashemi a , W.J. Lee b , C. Leinenbach, Recovery stress formation in FeMnSi based shape memory alloys: Impact of precipitates, texture and grain size, Materials and Design 2018
- [8] W. J. Lee, R. Partovi-Nia, T. Suter and C. Leinenbach\*, Electrochemical characterization and corrosion behavior of an Fe-Mn-Si shape memory alloy in simulated concrete pore solutions, Materials and Corrosion 2016
- [9] Zhizhong Dong, Ulrich E. Klotz, Christian Leinenbach\*, Andrea Bergamini, Christoph Czaderski, and Masoud Motavalli ,A Novel Fe-Mn-Si Shape Memory Alloy With Improved Shape Recovery Properties by VC Precipitation, Advanced Engineering Materials 2009
- [10] W J Lee, B Weber, G Feltrin, C Czaderski, M Motavalli and C Leinenbach , Stress recovery behaviour of an Fe–Mn–Si–Cr–Ni–VC shape memory alloy used for prestressing, Smart Materials and Structures 2013
- [11] W.J. Lee, B. Weber, G. Feltrin, C. Czaderski, M. Motavalli, C. Leinenbach, Phase transformation behavior under uniaxial deformation of an Fe–Mn–Si–Cr–Ni–VC shape memory alloy, Materials Science & Engineering 2013